ARTICLE

Journal of Materials Chemistry
www.rsc.org/materials

A facile liquid foam based synthesis of nickel nanoparticles and their subsequent conversion to $Ni_{core}Ag_{shell}$ particles: structural characterization and investigation of magnetic properties

Tanushree Bala, S. D. Bhame, P. A. Joy, B. L. V. Prasad* and Murali Sastry*

Materials Chemistry Division, National Chemical Laboratory, Pune 411 008, India. E-mail: sastry@ems.ncl.res.in; blvprasad@dalton.ncl.res.in

Received 8th April 2004, Accepted 11th August 2004
First published as an Advance Article on the web 2nd September 2004

A facile route for the synthesis of nickel nanoparticles in stable aqueous foams is reported. The Ni nanoparticles were roughly 12–15 nm in size and were stable as aqueous suspensions or powders when oleic acid was used as a capping agent. These Ni nanoparticles were subsequently coated with a silver shell in view of the extra stability and the enhanced manipulative ability afforded by the silver nanocoating. This was accomplished by a simple transmetallation reaction wherein the nanoparticle surface nickel atoms act as localized reducing agents for the silver ions in solution. As the silver shell is formed through the surface reaction a reduction in the average size of the Ni_{core} occurs. After the core–shell structure formation, the Ni_{core} has an average diameter of 10–20 nm while the Ag_{shell} has a thickness of 2–4 nm. The pristine oleic acid coated Ni and $Ni_{core}Ag_{shell}$ nanoparticles were probed for their magnetic characteristics by a vibrating sample magnetometer. The nascent, oleic acid coated Ni nanoparticles display a low superparamagnetic blocking temperature, T_B, of 20 K. The field dependent magnetic behaviour above and below T_B displays the standard features corresponding to superparamagnetism, as expected for very small Ni crystallites suggesting again that each 12 nm particle is polycrystalline. The magnetic contribution in the $Ni_{core}Ag_{shell}$ system comes from only the Ni core and predictably, the blocking temperature of this system is below 12 K due to the smaller size of the Ni core.

Introduction

Nanoscale magnetic particles are expected to be one of the key components in the nanotechnology revolution in the biological, electronic and catalytic arenas.[1] Depending on the mode of application the presence of nanomagnetic materials in different environments is preferred.[2] For example, in the electronic industry, dispersions of nanomagnetic materials in organic media might be essential due to the easy processability and excellent coating and drying capabilities of organic solvents. On the other hand, catalytic and biological applications require aqueous preparative procedures for these materials owing to the great synthetic flexibility and availability of greater access to bulk quantities of active materials.[3] Apart from this, for any biological or drug delivery application aqueous suspension is a prerequisite.[4]

Research on the synthesis of different types of magnetic nanomaterials is a major thrust area today. Excellent procedures are available to synthesize different nanomagnetic materials and great control over the size and shape has been achieved.[5] However, above 90% of these procedures are carried out in organic media and at relatively high temperatures especially if the methods pertain to single element magnetic materials like Fe, Co and Ni. Among these magnetic materials, cobalt based systems have received more attention probably due to their greater stability towards oxidation when compared to Fe and Ni systems.[6] Most of the literature concerned with Ni based nanoparticles is on support systems which were synthesized with their catalytic applications in view.[7] In fact, there are very few reports on the synthesis of free nickel nanoparticles in either aqueous or organic environments.[8]

We have reported on the use of a foam-based method for the synthesis of various nanomaterials.[9–11] The list of nanomaterials so far synthesized using this novel yet simple aqueous medium based route include metals,[9] minerals,[10] and oxides.[11] In this paper we report on the synthesis of Ni nanoparticles *via* this technique, their subsequent conversion to $Ni_{core}Ag_{shell}$ systems and their structural characterization and magnetic measurements. To our knowledge, this is the first totally aqueous based synthesis method at room temperature resulting in discrete nanoparticles of nickel that are not bound to a support. The typical foam-based synthesis of metal nanoparticles involves the following steps: 1) generation of a liquid foam from the mixture of metal salts and a suitable surfactant (if the metal is in cationic form then the surfactant taken is anionic and *vice versa*); 2) removal of excess liquid by drainage to get a dry foam, and 3) reducing the metal ions *in situ* by exposure of the foam to suitable reducing agents. While this general procedure works for most of the noble metal nanoparticles, for magnetic metal nanoparticles a slight modification of the procedure was required in the sense that we needed to take oleic acid along with the surfactant inside the foam matrix. We have observed that this leads to the immediate capping and stabilization of the metal nanoparticles with oleic acid as soon as they are formed in the foam.[9c]

In the dry foam condition the liquid volume fraction is at its minimum allowed limit and hence the liquid lamellae between the foam bubbles are very thin and possibly in the nanometer regime.[12] Therefore, any reaction happening in this restricted space would result in the restriction of the sizes of particles obtained. This is the reason why we observe nanometer sized particles when we carry out the reduction of Ni^{2+} ions in the foam matrix. The presence of oleic acid along with the foaming surfactant results in the immediate stabilization of the nanomaterials formed. The conversion of pure Ni to an $Ni_{core}Ag_{shell}$ system was accomplished by a simple transmetallation reaction.[13] This reaction occurs since the redox potentials of Ni^0 oxidation and Ag^+ reduction are such that $Ni^0 + 2Ag^+ \rightarrow Ni^{2+} + 2Ag^0$ is a spontaneous reaction and a simple mixing of Ni nanoparticles and Ag^+ ions resulted in a $Ni_{core}Ag_{shell}$ system capped by oleic acid. The presence of a silver shell capped with oleic acid gives the nickel nanoparticles an additional degree of freedom in that the $Ni_{core}Ag_{shell}$ nanoparticles could be readily transferred to a non-polar

DOI: 10.1039/b405335b

organic solvent.[14] This is in stark contrast to the behaviour of pure oleic acid capped nickel nanoparticles that did not undergo any phase transfer. This is one of the several advantages of the $Ni_{core}Ag_{shell}$ structure that we would like to highlight.

The magnetic characteristics of the pristine oleic acid capped Ni nanoparticles and their $Ni_{core}Ag_{shell}$ counterparts were investigated further. The magnetic properties reveal that the nickel nanoparticles display superparamagnetic characteristics with a blocking temperature of about 20 K. The magnetization *vs.* field curves above and below this blocking temperature again support the presence of superparamagnetism in these samples. Coating a thin silver shell around the Ni nanoparticles shifts the blocking temperature below 12 K. This is easily explained based on the fact that during the shell formation, a few layers of Ni atoms on the Ni core are consumed in the transmetallation reaction resulting in a reduction in the size of the Ni nanoparticles. Presented below are details of the investigation.

Experimental

Materials

Silver sulfate (Ag_2SO_4), sodium borohydride ($NaBH_4$), oleic acid (9-octadecenoic acid), nickel nitrate hexahydrate ($Ni(NO_3)_2{\cdot}6H_2O$) and sodium dodecyl sulfate (SDS) were purchased from Sigma Aldrich and used as received.

Preparation of Ni and $Ni_{core}Ag_{shell}$ nanoparticles

These nanoparticles are prepared by the foam based protocol which is explained in detail elsewhere.[9c] In a typical experiment, a rectangular column of 50 cm height and a square base of 10 × 10 cm^2 with sintered ceramic discs embedded in it was made using pyrex and was used for the generation of foam. An aqueous mixture of 50 ml of 1×10^{-3} M nickel nitrate solution, 10 ml of 1×10^{-3} oleic acid in methanol and 40 ml of 1×10^{-1} M SDS was placed in the base and the foam was built up by injecting nitrogen at a pressure of 1–5 psi through the porous ceramic disc fixed to the bottom of the foam column. Stable foams of up to 50 cm height could be routinely obtained. After carefully draining out the excess aqueous SDS/oleic acid + $Ni(NO_3)_2$ solution in the foam, the nickel ions in the foam were subjected to reduction by spraying sodium borohydride solution into the foam. As the nickel ions were reduced and nanoparticle formation progressed, the foam changed from gray to black and gradually collapsed. The collapsed foam solution containing the oleic acid capped Ni nanoparticles was collected through an outlet provided at the bottom of the column. This solution was then subjected to centrifugation at 5000 rpm for 30 minutes following which the pellet and supernatant were separated. The pellet was washed several times with ethanol before further characterizations were carried out. For the preparation of core–shell particles, the pellet of oleic acid-stabilized Ni nanoparticles (5 ml) after centrifugation was washed several times with ethanol and then dispersed in water. To this, 1 ml of 5×10^{-5} M Ag_2SO_4 solution was added. The color of the solution immediately changed to brownish yellow indicating formation of the Ag shell.

Measurements

UV-Vis spectroscopic studies

The optical properties of Ni_{core} and $Ni_{core}Ag_{shell}$ nanoparticle solutions were monitored on a Jasco UV-Vis spectrophotometer (V570 UV-VIS-NIR) operated at a resolution of 2 nm.

Fourier transform infrared (FTIR) spectroscopy measurements

FTIR spectra were recorded from drop-coated films of the nanoparticle samples deposited on Si (111) substrates on a Perkin Elmer Spectrum-One Spectrometer operated in the diffuse reflectance mode at a resolution of 4 cm^{-1}. The spectrum of pure oleic acid was also recorded for comparison.

Transmission electron microscopy measurements

TEM measurements were performed on a JEOL model 1200EX instrument operated at an accelerating voltage at 120 kV. Each sample was prepared from an aqueous suspension of the nanoparticles by placing a drop of the solution on a carbon-coated copper grid. The films on the TEM grids were allowed to dry for 2 min following which the extra solution was removed using a blotting paper.

X-Ray diffraction (XRD) measurements

XRD measurements of the Ni and $Ni_{core}Ag_{shell}$ nanoparticles were performed by casting the respective nanoparticle solutions in the form of films on glass substrates by simple solvent evaporation. The X-ray diffraction measurements were carried out on a Philips PW 1830 instrument operating at 40 kV and a current of 30 mA with Cu K_α radiation.

Thermogravimetric analysis (TGA)

TGA analyses of the dried Ni and $Ni_{core}Ag_{shell}$ powders were done on a TGA-7 Perkin Elmer instrument in the temperature range 30–800 °C at a scan rate of 10 °C min^{-1}.

Magnetic measurements

The magnetic characteristics of the Ni and $Ni_{core}Ag_{shell}$ nanoparticle powder samples were measured using a EG&G PAR 4500 vibrating sample magnetometer. Zero-field-cooled (ZFC) magnetization curves were obtained after cooling the sample from room temperature to 12 K without any external magnetic field and then measuring the magnetization while warming the sample under an external field of 50 Oe. For field-cooled (FC) measurements, the sample was cooled to 12 K under an external field of 50 Oe and the magnetization was measured while warming in the same field. Magnetization as a function of magnetic field was measured by varying the field between −10000 Oe and 10000 Oe, at different temperatures in the range 12–300 K.

Results and discussion

As mentioned briefly in the introduction, we carry out reduction of metal ions inside the foam matrix after draining the excess liquid. This often leads to very stable dry foams where the bubbles generally tend to assume polyhedral shapes. In this condition, the dihedral angles where three faces of the bubbles meet are around 120° and those where four faces meet are around 109°. This confirms that we are at the dry limit of the foam and these features along with the high stability of the dry foam suggest that the foam is in its mechanical equilibrium geometry. In this scenario the liquid lamellae between the faces of the bubbles are very thin and the regions between these surfactant layers where the metal ions are encapsulated are probably in the range of few nanometers.[12] In actual experiments, we have two surfactants present in the system, namely SDS and oleic acid. Both are anionic surfactants and due to purely entropic considerations we can expect that both SDS and oleic acid are present in these lamellar layers complexed to the Ni^{2+} ions. As the Ni^{2+} ions are being reduced, it is expected that the oleic acid binds to the nascent Ni nanoparticles thereby stabilizing them *in situ*. The TEM images of the nickel nanoparticles thus prepared are displayed in

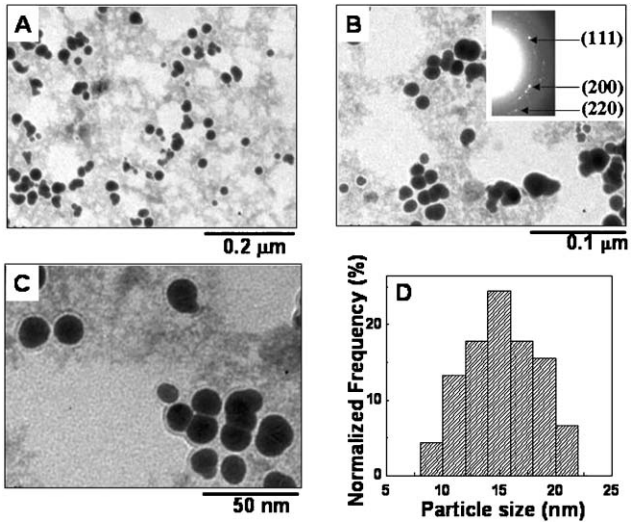

Fig. 1 A–C: Representative TEM images of Ni nanoparticles from several areas of the grid. The selected area diffraction and the indexing of the rings to the fcc phase of nickel are provided in the inset of B. Note the diffuse spot pattern obtained (see text for more details). The particle size distribution (D) reveals the average size to be around 12–15 nm.

Fig. 1A–C. It is clear from the TEM images that the Ni nanoparticles prepared by the above procedure are polydisperse in nature with an average size of 12–15 nm (Fig. 1D). The selected area electron diffraction pattern (SAED) from these nanoparticles revealed a diffuse ring structure with spots superimposed (inset of Fig. 1B). This suggests that the nanoparticles formed are quite polycrystalline. The *d* values calculated from the positions of the electron diffraction rings agreed well with the *d* values reported for *fcc* Ni. It is worth noting here that no diffraction patterns corresponding to nickel oxides were observed. We could not get good X-ray diffraction patterns from Ni nanoparticle samples possibly due to the small size of the Ni crystallites. The nickel particles are capped by oleic acid as they are being formed in the foam matrix and this could be the reason for the extra stability of Ni nanoparticles against oxidation in the aqueous dispersion form as well as in the powder form.

The TEM images of the $Ni_{core}Ag_{shell}$ system are presented in Fig. 2A–C. The particles clearly show a dark core capped with a lighter shell indicating the formation of a $Ni_{core}Ag_{shell}$ structure. The core–shell structure is more clearly seen in the

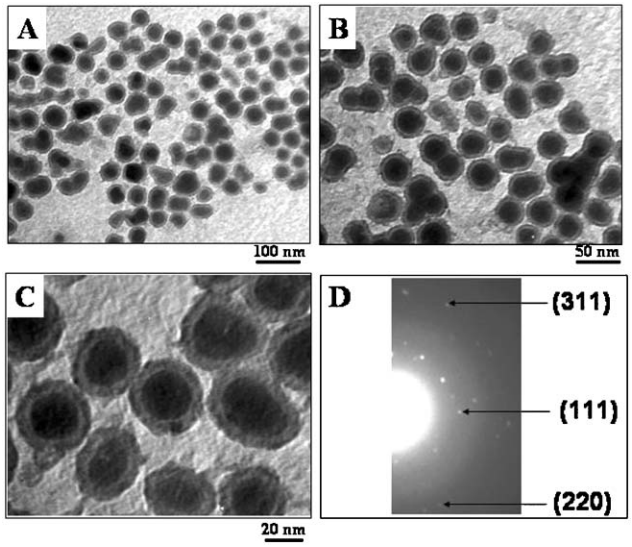

Fig. 2 A–C) Representative TEM images of the $Ni_{core}Ag_{shell}$ system. D) SAED diffraction pattern from the $Ni_{core}Ag_{shell}$ nanoparticles with rings indexed with respect to *fcc* silver.

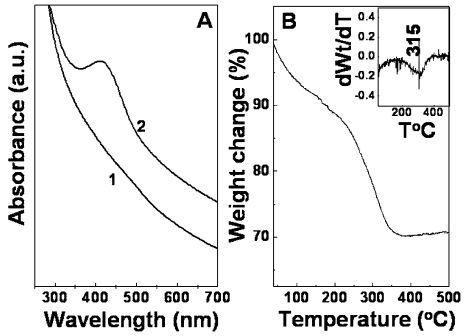

Fig. 3 (A) UV-Vis spectra of Ni (curve 1) and $Ni_{core}Ag_{shell}$ nanoparticle dispersion in aqueous medium (curve 2). (B) TGA curve of the oleic acid capped nickel nanoparticles. The inset in B is the first derivative of the weight loss curve indicating that the maximum of weight loss occurs at 315 °C.

highest magnification image (Fig. 2C). The core–shell particles range in size from 15–30 nm, the increase in average size measured with respect to the Ni nanoparticles providing further proof for deposition of an Ag shell on the Ni particles. The SAED pattern recorded from the $Ni_{core}Ag_{shell}$ nanoparticles is shown in Fig. 2D. The pattern is characteristic of polycrystalline particles and the rings could be indexed with reference to the *fcc* silver structure. This indicates that the shell is reasonably thick (as inferred from the TEM images) and prevents penetration of the electron beam to the Ni core. The UV-Vis spectrum of the pristine oleic acid capped Ni nanoparticles (Fig. 3A, curve 1) is almost featureless with a monotonic increase in the absorbance with decrease in wavelength and agrees well with those reported for Ni nanoparticles.[15] The development of a surface plasmon resonance peak around 415 nm attributed to silver in the nanoscale regime is observed once the transmetallation reaction is carried out (Fig. 3A, curve 2). This result, along with the contrast difference in TEM images, clearly suggests that a silver shell is formed around the Ni core. The formation of a silver shell is also confirmed indirectly from the magnetic measurements where a shift in the blocking temperature to lower values is observed after the shell formation (*vide infra*).

Thermogravimetric analysis was carried out to determine the amount of capping agent (oleic acid) present per gram of the sample. As shown in Fig. 3B the pristine oleic acid capped Ni nanoparticles show a small weight loss at around 100 °C (probably due to loss of water) that is followed by a more significant weight loss of about 18% around 315 °C. This weight loss is attributed to the desorption/decomposition of oleic acid present on the surface of the Ni nanoparticles. Assuming that the oleic acid forms a close packed monolayer on the surface of the Ni nanoparticle and an area per carboxylic unit of roughly 21.4 $Å^2$ (ref. 16), each nanoparticle would be covered by 2000–3250 molecules of oleic acid for the 12–15 nm particles. This translates into roughly 10–12 weight% of oleic acid. Our TGA analysis shows that there is a slight excess of oleic acid on the surface compared with what was expected. A number of factors such as uncertainty in the nanoparticle surface area due to polydispersity could contribute to this discrepancy. Such results have been observed earlier for ligands capping nanoparticle surfaces and have been explained on the basis of either smaller areas occupied by the ligand on the nanoparticle surface or the due to the presence of excess ligand at interstitial sites of nanoparticle aggregates.[17]

The temperature dependence of the magnetic susceptibility for the Ni and $Ni_{core}Ag_{shell}$ nanoparticles are shown in Fig. 4A and B, respectively. In all the cases, the applied magnetic field was 50 Oe and the temperature was varied between room temperature and 12 K. Curve 1 in Fig. 4A corresponds to the susceptibility *vs.* temperature plot for the pristine Ni system in

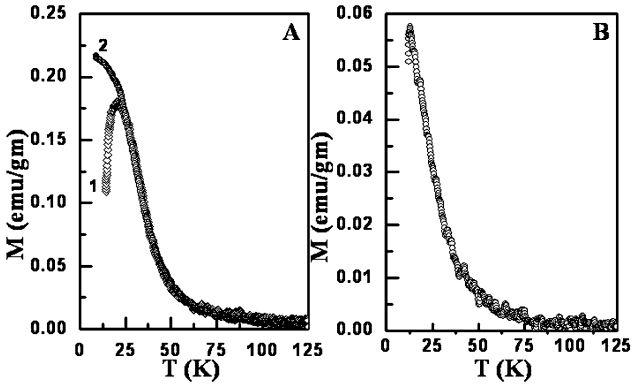

Fig. 4 (A) Temperature dependent magnetization of nickel nanoparticles in the zero field cooled (ZFC, curve 1) and field cooled (FC, curve 2) modes. The divergence between the two curves at 20 K is related to the blocking temperature. The applied magnetic field was 50 Oe. (B) The temperature dependent magnetization of the $Ni_{core}Ag_{shell}$ nanoparticles under the same external field.

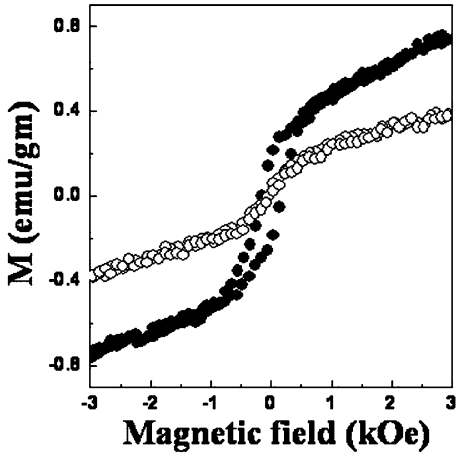

Fig. 5 Field dependent magnetization of Ni nanoparticles below (●, 12 K) and above (○, 60 K) the blocking temperature.

the zero-field-cooled (ZFC) mode while curve 2 is the measurement carried out in the field-cooled (FC) mode. As can be clearly seen, the curves of temperature dependent ZFC and FC susceptibilities are typical of magnetic nanoparticles. Magnetic particles below a certain size regime behave as superparamagnetic particles. The features characteristic of superparamagnetic particles are: i) the zero-field-cooled DC susceptibility, measured using very low magnetic fields, displays a maximum in the susceptibility at a certain temperature, called the blocking temperature, T_B; ii) a divergence in the ZFC and FC susceptibility curves below the blocking temperature and iii) magnetic hysteresis loop and remnant magnetization below T_B whereas the magnetic hysteresis behavior disappears above T_B. For the pristine oleic acid capped nickel nanoparticles, the ZFC curve shows a maximum at 20 K and the ZFC and FC curves show a divergence below this temperature revealing that the blocking temperature is 20 K. The blocking temperature is actually related to the size of the magnetic particles and the magnetocrystalline anisotropy constant (K) by the equation $K = 25k_BT_B/V$ where k_B and V are the Boltzmann constant and the volume of a single particle, respectively and T_B is the blocking temperature. By substituting the values for a 12 nm particle we deduce K to be 0.76×10^5 erg cm^{-3}, which is comparable to that of bulk nickel (0.5×10^5 erg cm^{-3}).[18] The small difference between the values is expected as we calculated K using the average particle size and not the individual crystallite size which actually controls the individual magnetic directions of the grains and hence the blocking temperature. Apart from this, several other phenomena related to the nanoscale regime such as the structural disorder, surface anisotropy, non-magnetic or weak magnetic interfaces, the lack of surface coordination for the surface magnetic atoms and the electron exchange between the capping agent and surface atoms are also known to influence the magnetic properties.[8d] One or several of these phenomena in tandem could also have led to the smaller values of the magnetic characteristics in our systems.

The field dependent magnetic behavior data, measured at 12 K (below the blocking temperature, curve 1) and at 60 K (well above the blocking temperature, curve 2) are displayed in Fig. 5. Again, the features observed in the M–H curves are in accordance with those expected for superparamagnetic particles, *i.e.* i) no saturation was observed in the magnetization even at very high fields (actually up to our instrument limit); ii) magnetic hysteresis with a coercivity of 160 Oe and remnant magnetization below the blocking temperature and iii) disappearance of magnetic hysteresis above the blocking temperature. All these features suggest again that the oleic acid capped nickel nanoparticles prepared by the foam technique indeed behave as superparamagnetic particles.

The curve in Fig. 4B is the temperature dependence of ZFC magnetization observed for the $Ni_{core}Ag_{shell}$ nanoparticle sample. The silver shell around the Ni nanoparticles is formed by a transmetallation reaction wherein a few layers of the surface nickel atoms are oxidized to Ni^{2+} in the process of reducing silver ions. This reduces the average particle size of nickel. Since the as-prepared nickel nanoparticles are polydisperse in nature we observe a polydispersity in the core–shell structures also with the average size of the $Ni_{core}Ag_{shell}$ particle in the range of 15–30 nm comprising a core of 10–20 nm size. In general the blocking temperature is expected to shift to lower temperatures as the particle size is reduced. Accordingly, no maximum in the ZFC susceptibility or no divergence between the ZFC and FC susceptibilities is observed down to 12 K (compared to $T_B = 20$ K for the 12 nm Ni particles) indicating that the blocking temperature is now shifted to below 12 K (the lower limit of our cryostat) which could be attributed to the reduced Ni core size. In fact, the blocking temperature of the 10 nm sized Ni nanoparticles is calculated as ~11 K from the relation $T_B = KV/25k_B$, by using the deduced value of $K = 0.76 \times 10^5$ erg cm^{-3} for the 12 nm Ni particles.

Conclusions

An easy foam based method for the synthesis of nickel based nanoparticulate systems is reported. This is probably the first method for a completely water-based synthesis of nickel nanoparticles at room temperature. The magnetic characteristics of the nickel nanoparticles are in accordance with those expected for nanoscale superparamagnetic particles. The blocking temperature where the magnetic directions of individual grains essentially remain invariant was determined to be 20 K for the oleic acid capped nickel particles. The nickel nanoparticles were easily converted to $Ni_{core}Ag_{shell}$ nanoparticulate structures following a transmetallation reaction. The blocking temperature was shown to be shifted to lower temperatures upon silver shell formation. Further studies where the nanoparticle size could be controlled to different sizes and variation of shell thickness are in progress.

Acknowledgements

BLVP thanks the National Chemical Laboratory for a start-up grant. TB acknowledges a Junior Research fellowship from CSIR, Govt. of India. The TEM and SEM analyses were carried out at the Center for Materials Characterization (CMC), NCL Pune and are gratefully acknowledged.

References

1 (*a*) D. D. Awschalom and D. P. DiVincenzo, *Phys. Today*, 1995, **48**, 43; (*b*) J. Shi, S. Gider, K. Babcock and D. D. Awschalom, *Science*, 1996, **271**, 937; (*c*) C. M. Sorensen, in *Nanoscale Materials in Chemistry*, ed. K. J. Klabunde, Wiley, New York, 2002, p. 169.

2 M. Sastry, in *The Chemistry of Nanomaterials*, ed. C. N. R. Rao, A. Muller and A. K. Cheetham, Wiley-VCH, Weinheim, 2004, ch. 3, p. 31.

3 R. Schlögl and S. B. Abd Hamid, *Angew. Chem., Int. Ed.*, 2004, **43**, 1628–1637.

4 P. Tartaj, M. P. Morales, S. V.- Verdaguer, T. G.- Carreno and C. J. Serna, *J. Phys. D: Appl. Phys.*, 2003, **36**, R182–R197.

5 For a general review of synthesis of magnetic nanoparticles see, T. Hyeon, *Chem. Commun.*, 2003, 927–934.

6 (*a*) C. B. Murray, S. Sun, W. Gaschler, H. Doyle, T. A. Betley and C. R. Kagan, *IBM J. Res. Dev.*, 2001, **45**, 47; (*b*) C. B. Murray, S. Sun, H. Doyle and T. A. Betley, *MRS Bull.*, 2001, 985; (*c*) S. Sun and C. B. Murray, *J. Appl. Phys.*, 1999, **85**, 4325; (*d*) M. R. Diehl, J.-Y. Yu, J. R. Heath, G. A. Held, H. Doyle, S. Sun and C. B. Murray, *J. Phys. Chem. B*, 2001, **105**, 7913; (*e*) Z. L. Wang, Z. Dai and S. Sun, *Adv. Mater.*, 2000, **12**, 1944; (*f*) D. P. Dinega and M. G. Bawendi, *Angew. Chem., Int. Ed.*, 1999, **38**, 1788; (*g*) V. F. Puntes, K. M. Krishnan and A. P. Alivisatos, *Appl. Phys. Lett.*, 2001, **78**, 2187; (*h*) C. T. Black, C. B. Murray, R. L. Sandstrom and S. Sun, *Science*, 2000, **290**, 1131; (*i*) C. Petit, T. Cren, D. Roditchev, W. Sacks, J. Klein and M. P. Pileni, *Adv. Mater.*, 1999, **11**, 1198; (*j*) M. P. Pileni, *Langmuir*, 1997, **13**, 3266; (*k*) J. P. Chen, C. M. Sorensen, K. J. Klabunde and G. C. Hadjipanayis, *J. Appl. Phys.*, 1994, **76**, 6316; (*l*) C. Petit, A. Taleb and M. P. Pileni, *J. Phys. Chem. B*, 1999, **103**, 1805; (*m*) C. Petit, A. Taleb and M. P. Pileni, *Adv. Mater.*, 1998, **10**, 259; (*n*) K. S. Suslick, M. Fang and T. Hyeon, *J. Am. Chem. Soc.*, 1996, **118**, 11960; (*o*) K. S. Suslick, T. Hyeon and M. Fang, *Chem. Mater.*, 1996, **8**, 2172; (*p*) K. V. P. M. Shafi, A. Gedanken and R. Prozorov, *Adv. Mater.*, 1998, **10**, 590; (*q*) T. Hyeon, S. S. Lee, J. Park, Y. Chung and H. B. Na, *J. Am. Chem. Soc.*, 2001, **123**, 12798; (*r*) S.-W. Kim, S. U. Son, S. S. Lee, T. Hyeon and Y. K. Chung, *Chem. Commun.*, 2001, 2212.

7 K. Matsuo and K. J. Klabunde, *J. Org. Chem.*, 1982, **47**, 843 and Ni on support systems.

8 (*a*) G. N. Glavee, K. J. Klabunde, C. M. Sorensen and G. C. Hadjipanayis, *Langmuir*, 1994, **10**, 4726; (*b*) P. D. Hooker and K. J. Klabunde, *Chem. Mater.*, 1993, **5**, 1089; (*c*) T. Hou and S. Gao, *J. Mater. Chem.*, 2003, **13**, 1510; (*d*) D. H. Chen and S. H. Wu, *Chem. Mater.*, 2000, **12**, 1354; (*e*) M. Green and P. O'Brien, *Chem. Commun.*, 2001, 1912.

9 (*a*) S. Mandal, S. K. Arumugam, S. D. Adyanthaya and M. Sastry, *J. Mater. Chem.*, 2004, **14**, 43; (*b*) S. Mandal, S. K. Arumugam, R. Pasricha and Murali Sastry, *Appl. Nanosci.* in press; (*c*) T. Bala, S. K. Armugam, R. Pasricha, B. L. V. Prasad and M. Sastry, *J. Mater. Chem.*, 2004, **14**, 1057.

10 D. Rautaray, K. Sinha, S. Shiv Shankar, S. D. Adyanthaya and M. Sastry, *Chem. Mater.*, 2004, **16**, 1356.

11 S. Shivshankar, U. Patil, B. L. V. Prasad and M. Sastry, *Langmuir*, submitted.

12 (*a*) J. A. F. Plateau, *Statique Experimentale et Theorique des Liquides*, Gauthier-Villiard, Paris, 1873; (*b*) J. E. Taylor, *Ann. Math.*, 1976, **103**, 489.

13 J.-Il. Park and J. W. Cheon, *J. Am. Chem. Soc.*, 2001, **123**, 5743.

14 (*a*) W. Wang, S. Efrima and O. Regev, *Langmuir*, 1998, **14**, 602; (*b*) W. Wang, X. Chen and S. Efrima, *J. Phys. Chem. B*, 1999, **103**, 7238.

15 J. A. Creighton and D. G. Eadon, *J. Chem. Soc., Faraday Trans. 1*, 1991, **87**, 3881.

16 A. Ulmann, *An Introduction to Ultra Thin Organic Films: From Langmuir–Blodgett to Self Assembly*, Academic Press, San Diego, 1991.

17 A. Badia, S. Singh, L. M. Demers, L. A. Cuccia, G. R. Brown and G. R. R. B. Lennox, *Chem. Eur. J.*, 1996, **2**, 205.

18 B. D. Cullity, *Introduction to Magnetic Materials*, Addison-Wesley Publishing, Reading, MA, 1972.